

LARGE-EDDY SIMULATION OF FLOW AND DISPERSION IN AN HETEROGENEOUS URBAN AREA: COMPARISON WITH FIELD DATA

Vera Rodrigues^{1,4}, Isabelle Calmet^{2,4}, Mirvatte Francis^{3,4}, Denis Maro^{3,4}, Didier Hébert^{3,4}, Olivier Connan^{3,4}, Philippe Laguionie^{3,4}, Magdalena Maché^{2,4}, Thibaud Piquet^{1,4}, Pascal Kéravec^{1,4} and Jean-Michel Rosant^{1,4}

¹LUNAM Université, CNRS, LHEEA UMR CNRS 6598, Nantes, France

²LUNAM Université, Ecole Centrale de Nantes, LHEEA UMR CNRS 6598, Nantes, France

³Laboratoire de Radioécologie de Cherbourg-Octeville (LRC), IRSN, Cherbourg, France

⁴Institut de Recherche en Sciences et Techniques de la Ville (IRSTV), FR CNRS 2488, Nantes, France

Abstract: An accurate atmospheric modelling at several neighbourhoods scale requires high resolution models, which must be suitable for the study of dispersion in heterogeneous urban canopies. With that purpose, a model for the scalar dispersion simulation within and above the canopy has been developed where transport-diffusion equation is solved. In the present study, we use the large-eddy simulation atmospheric model ARPS (Advanced Regional Prediction System), in which the influence of the urban canopy on flow and turbulence is modelled with a drag-force approach.

In the framework of the federative project VegDUD, two experimental campaigns of urban climatology measurements FluxSAP (May 2010 and June 2012) have been carried out in a suburban district of Nantes (France). Several release experiments using SF₆ as a gas tracer were performed during these periods, as well as local measurements of the meteorological variables such as wind and turbulence.

This paper presents the model application to this real urban canopy and the comparison between numerical results and experimental wind flow and dispersion data available from the FluxSAP database.

Key words: Large-eddy simulation, atmospheric flow, dispersion, heterogeneous urban area.

INTRODUCTION

Modelling turbulent flow and scalar transfers between the urban canopy and the atmosphere is of great importance to better understand the influence of the urban morphology on the microclimate and on the characteristics of pollutant dispersion. Nowadays, pollutant dispersion in urban areas represents a major concern, mainly due to its impact on human health. Depending on the scale at which the dispersion is studied, several approaches are available and can be used to simulate flow and scalar fields. Typically, the widely applied building resolving CFD models are well suited for street or small neighbourhood scales, while atmospheric models in which the surface is represented as a patchwork of roughness are usually used at regional or city scales. High resolution atmospheric models dealing with an intermediate scale of several neighbourhoods must be suitable for the dispersion study in heterogeneous urban areas, providing a powerful tool for an accurate evaluation of pollutant dispersion. In this paper, we propose to use the large-eddy simulation atmospheric model ARPS (Advanced Regional Prediction System) for the passive tracer concentration modelling.

Despite recent advances in the atmospheric modelling, identifying and reducing uncertainties remains a challenge. Hence, several experimental campaigns have been carried out throughout the last decades in order to assess these models and to improve our knowledge of the urban atmospheric flows. In this context, the FluxSAP 2010 and 2012 experimental campaigns have been carried out with the main purpose of assessing the accuracy of different numerical models in real urban configurations.

The data of the FluxSAP 2010 campaign thoroughly described in Maro et al. (2011) have been already used in several studies. Francis et al. (2012) compared SF₆ dispersion measurements to the results of the Briggs' urban Gaussian model under several atmospheric stability conditions. They demonstrated a good agreement between experimental and simulated horizontal and vertical plume widths. Rodrigues et al. (2012) have shown some preliminary results concerning the application of the ARPS model, with the dispersion computation, to this experimental set and have found a significant underestimation of the simulated concentration, explained by the differences between experimental and meteorological conditions. Regarding the dynamics of the flow in terms of mean wind speed and direction, the ARPS model including the drag-force approach developed by Maché et al. (2012) has been tested over the FluxSAP experimental site under neutral conditions and for steady westerly wind. This approach reproduces the influence of the neighbourhood morphological heterogeneity on the flow field inside and above the canopy layer. The numerical results were used among other approaches by Borrego et al. (2012) in order to define the inflow conditions to be set at the boundaries of the micro-scale model VADIS, thereby evaluating the model sensitivity for dispersion simulation to different methods of deriving the inflow vertical wind profiles in urban areas. This analysis has demonstrated that the ARPS model properly takes into account the upwind urban area characteristics, providing reliable inflow conditions, even if all the methods lead to an overestimation of the SF₆ concentration.

In this paper we discuss the ARPS model efficiency to directly simulate the dispersion during one of the SF6 releases of the FluxSAP 2010. The model is assessed by means of comparison between numerical results and experimental data.

MODEL DESCRIPTION

The large-eddy simulation atmospheric model, ARPS, has been modified to compute the influence of urban canopies on the flow dynamics and the turbulence by applying a drag force-approach (Maché et al., 2010). The urban canopy is described by averaged morphological parameters such as frontal and surface densities, and mean and maximal buildings height. Furthermore, ARPS is adapted to compute the passive tracer concentration within and above the urban canopy (Rodrigues et al., 2012) by solving the scalar diffusion-transport equation:

$$\frac{\partial \bar{C}}{\partial t} + \frac{1}{G} \frac{\partial G u_i \bar{C}}{\partial x_i} = \frac{1}{G} \frac{\partial G q_i^{SGS}}{\partial x_i} + \frac{1}{G} S_C, \quad (1)$$

Where *overbars* denote resolved instantaneous fields, u_i represents each velocity component (u, v, w) and x_i the spatial coordinates (x, y, z). The time evolution of the passive tracer C results from the balance between advection by turbulent flow, subgrid-scales fluxes (q_i^{SGS}) and the sources in the domain. The advection and the subgrid-scale schemes are discussed in Rodrigues et al. (2012). The emission source is defined as a volume source in a computational grid. Nevertheless, we consider that an emission source defined in a grid represents a punctual emission, therefore punctual, line and surface sources can be treated. Moreover, we are able to define an emission release in time, during the entire period of simulation or during parts of this period. The presence of buildings, specifically in the concentration module, is taken into account in each grid of the computational domain with variable G , which point out the ratio between the air volume and the total grid volume.

SIMULATION DETAILS

Several simulations were carried out in the real urban configuration in order to reproduce one of the releases of the experimental campaign FluxSAP 2010. The experimental set selected to the comparison analysis is reported to the 26th May 2010 that is characterized by a low pressure system. The release was selected based on various criteria such as distance between emission and measurement, wind steadiness during the period and quasi-neutral atmospheric conditions.

The computational domain size is 2860 m x 3060 m x 1400 m, with 143 x 153 x 59 grids. The horizontal grid size is 20 m, while the vertical grid size is 1 m inside the canopy layer and up to 25 m. The vertical mesh is stretched above the 25 m level, with a mean value of 25 m. The time step is fixed at 0.03 s. The boundary conditions applied to the flow dynamics and turbulence are defined by external files, resulting from the grid nesting procedure, and zero normal gradients for all boundaries on the concentration field.

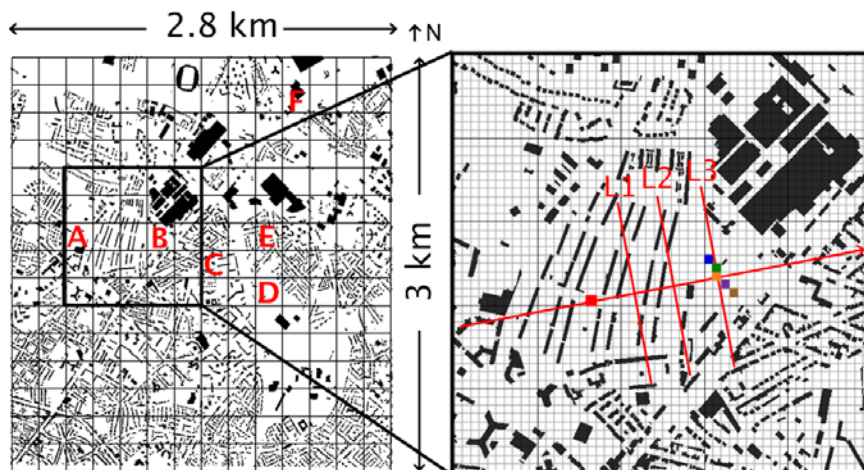


Figure 1. Simulation domain extracted with OrbisGIS from the French urban database BDTopo. The left side of the figure indicates the entire domain including the meteorological measurement locations. The right side shows an enlargement over the emission/ measurement region. From north to south, blue, green, yellow, violet and brown squares denote the computational grids corresponding to the Diapeg 1, 2, AA, 3 and 4, respectively. L1, L2 and L3 indicate the spanwise lines chosen to characterize the plume expansion (see Figures 2 and 3), located at 100 m, 200 m and 300 m from the release point, respectively. The red arrow perpendicular to the 3 lines represents the wind direction and the theoretical mean plume axis.

The turbulent flow reaches a statistically steady state after 6 eddy turnover times which corresponds to 12000 s. Thereafter, the passive tracer is released continuously from one grid (20 m x 20 m x 1 m) located above the ground, during 10 min with an emission rate of 5.3 g.s⁻¹. The release conditions are the same in the simulation as in the measurement setup. A detailed description of the experimental campaign is presented in Maro et al. (2011) and Francis et al. (2012).

The meteorological variables were measured at different heights on several meteorological masts. Figure 1 shows the entire simulation domain (left side) with indication of the meteorological measurement points (A=SEVE, B=Goss, C=Dunant, D=Eolienne, E=Maraiches, F=SG). The area including emission and measurement devices is enlarged (right side) showing the emission cell (red square) and the cells where concentration is measured. The measurement area is located at 300 m from the release point, approximately.

RESULTS DISCUSSION

The analysis of the simulations is carried out regarding the spanwise plume profiles. Figure 2a provides the plume profiles for the 3 lines perpendicular to the simulated mean wind direction, indicating the plume behaviour as a function of the distance from the release. Figure 2b shows the concentration profiles in the plume corresponding to line L3 that crosses the concentration measurement area. At 2.5 m above ground level (a.g.l.), the maximum concentration value is found at the Diapeg AA location (distance x = 0 m on Figure 2b), while at 4.5 m and 7.5 m a.g.l. this maximum is located in the grid corresponding to the Diapeg 3 (distance x = 20 m). Figure 2b also shows that the concentration maximum is registered at 4.5 m a.g.l. but varies of less than 10 µg.m⁻³ compared with the value at the ground level. Between 1.5 m and 7.5 m a.g.l. the plume width is 300m and it is mostly filled near the ground with maximum concentration values due to spanwise dispersion processes. On the contrary, for lines L1 and L2 the maximum values remain concentrated around the plume axis which slightly turns clockwise with the increased distance from the emission source (Figure 2a). These results illustrate the plume expansion in the spanwise direction with increased distances from the release.

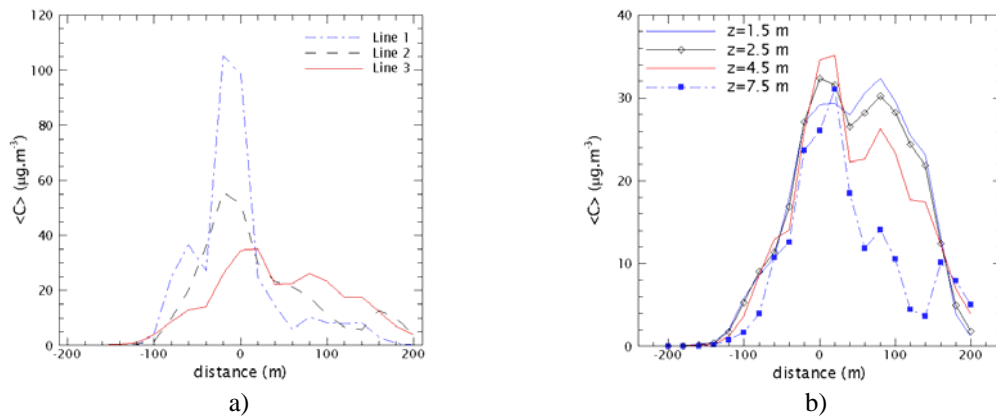


Figure 2. Spanwise plume profiles a) for the 3 lines (L1, L2 and L3) presented in Figure 1, at 4.5 m a.g.l., and b) for the line L3 at different levels. The axis of abscissas is aligned with the lines (L1 to L3) and positive in the NW-SE direction. The axis origin (x = 0 m) corresponds to the theoretical maximum concentration.

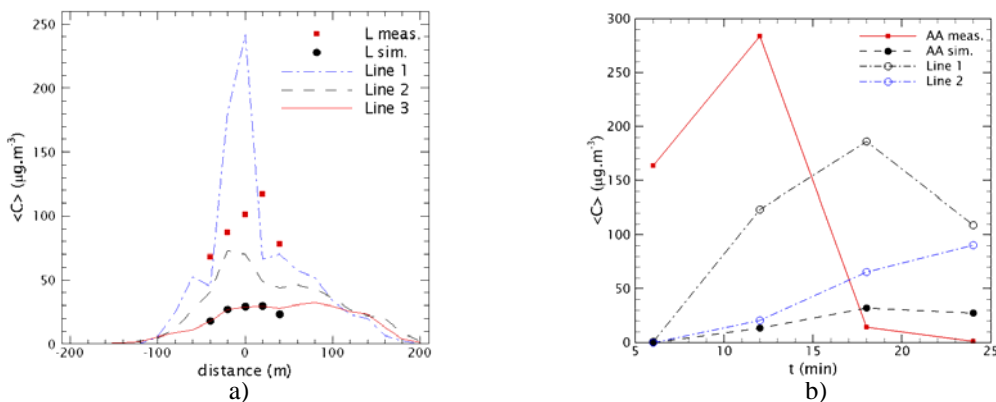


Figure 3. a) Spanwise plume profiles for the 3 lines at 1.5 m a.g.l., and for the line (L) of the measurement equipment (the averaging time is 24 min). b) Transit time of the experimental and simulated plume at the AA location and for the lines L1 and L2 at the computational grid with the maximum concentration value (each value corresponds to a 6 min time-averaging).

The FluxSAP database includes different sets of concentration data, such as instantaneous and time-averaged values. The plume arrival at the measurement site is determined by real time measurements (each 2 min) of SF6, providing the instantaneous concentration data (Maro et al., 2011). The mean values are determined by performing either a time-averaging during the entire period of measurement (24 min) or four consecutive 6 minutes time-averaging. Figure 3a presents the spanwise plume profiles for the 3 lines at the ground level (emission/ measurement level) together with the experimental values in order to compare measured (L meas.) and simulated (L sim.) mean concentrations for the 24 min averaging. Figure 3b shows the transit time of the experimental and simulated plume deduced from 6 min averaging. In addition, is also presented the transit time of the plume for the lines L1 and L2, considering the computational grid where the maximum concentration value is observed. Both measurements and simulations indicate that the plume axis passes through the Diapeg 3 and AA (Figure 3a). However, the point-to-point comparison shows that the concentration values are underestimated by factors 3 and 4 in the simulation. Mean concentration values matching with experimental data are simulated closer to the emission source point, near line L2. The differences between the concentration values obtained on lines L1 and L2 are larger than between lines L2 and L3, which might indicate an accumulation of the tracer in the vicinity of the emission source and explain the disagreement between measured and simulated concentrations. The accumulation issue is due to the location of the release very near the ground inside the canopy, where the wind velocity is weak.

Figure 3b presents a more detailed analysis useful to understand the deviations revealed on Figure 3a. In the experimental dataset mean concentration values at 6 min time-average are only available for the AA point, thus the comparison between numerical and experimental results is only performed for the Diapeg AA corresponding grid cell. The results exhibit the transit time of the experimental and simulated plumes. We observe that the experimental plume goes over the measurement site during the first 18 min while the simulated plume reaches the measurement area at least 6 minutes late, and stays in the area after the end of the simulation period, as also observed at the lines L1 and L2. From the results presented in Figures 3a and 3b we can state that the simulated plume is characterized by both space- and time-shift compared with the experimental plume.

As the flow dynamics governs the dispersion processes, a detailed analysis of the flow is indispensable for model assessment. A direct comparison between measured and simulated mean wind speed and direction averaged over 24 min is presented in Table 1 at the locations indicated in Figure 1. The wind directions are in good agreement, the differences ranging from 2° to 32° and the maximal deviation being observed at SEVE (14 m). The wind speed values are also in a good agreement varying from a perfect match at Dunant to a maximum deviation of 1.3 m.s⁻¹ at SG (32 m). From this analysis, we can conclude that the model presents a good performance regarding the mean flow, as previously shown by Maché et al. (2012). The Table 1 also shows that during the measurement period the wind blows from W-SW with a moderate speed, in accordance with the plume orientation.

Table 1. Comparison between the meteorological variables, wind speeds (WS) and directions (WD), measured (_{meas.}) and simulated (_{sim.}) for the different measurement sites.

	SEVE (14m)	SEVE (20m)	Goss (21m)	Goss (26m)	Dunant (15m)	Eolienne (10m)	Maraiches (10m)	SG (32m)
WS _{meas.} (m.s ⁻¹)	2.1	2.7	2.7	3.1	2.1	2.1	2.9	4.1
WS _{sim.} (m.s ⁻¹)	1.6	2.1	2.5	2.8	2.1	1.4	1.9	2.8
WD _{meas.} (°)	231	256	261	263	275	260	269	255
WD _{sim.} (°)	263	264	266	265	260	271	266	267

The time evolutions of wind speed and direction at Goss site (21 m) during the whole period are presented in Figure 4. The data have been averaged over short time (1 min) in order to highlight the wind variability in both simulation and experiment. During the measurement period a significant variability of the wind speed is recorded on site. The disagreements between measured and simulated wind speed and direction were not expected from the results shown in Table 1. For the first 5 minutes the simulated wind speeds are strongly underestimated, reaching a maximum deviation of 2.3 m.s⁻¹. This result can explain the time-shifting of the simulated plume previously discussed (Figure 3). In contrast, some periods of simulation show a wind speed overestimation with a maximum deviation of 0.8 m.s⁻¹. During half of the entire simulation period a difference less than 0.5 m.s⁻¹ is registered, in accordance with the results obtained by means of longer time averaging (Table 1). The statistical parameters suitable for the evaluation of the results accuracy were determined for the wind speed (24 pairs): the mean bias error (MBE) is equal to -0.5 m.s⁻¹ and the root-mean-square error (RMSE) is about 0.93 m.s⁻¹ which is a quite good score. Given the good performance of the model for the averaged flow

field, it seems that the discrepancies between experimental and numerical results for the concentration values are mostly related to the flow unsteadiness which is difficult to reproduce in the simulation.

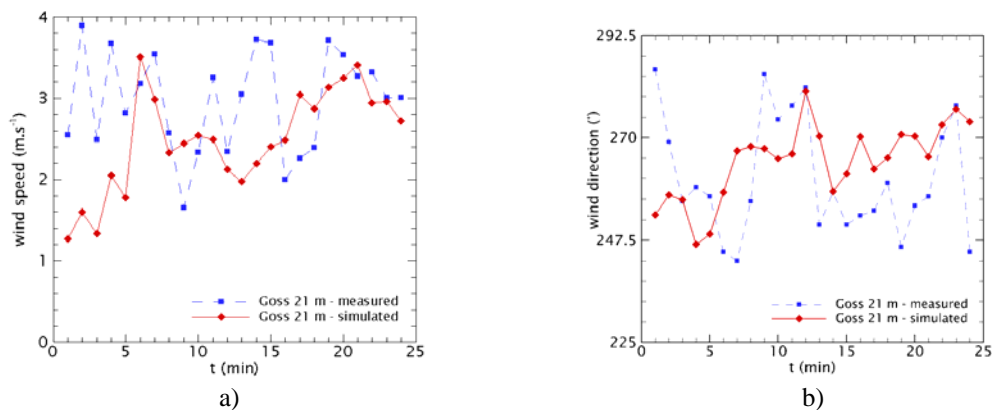


Figure 4. Comparison between wind speeds and directions simulated and measured at Goss site (point B in Figure 1), at level 21 m. These values are obtained with an average time of 1 min.

CONCLUSIONS

In this study, we discussed the comparison between measured concentration in a real urban site and the values simulated with the large-eddy simulation model ARPS. We noticed a systematic underestimation of the simulated concentration. The numerical results show a shift in time and space compared with the experimental plume. The 24 min time-averaged wind variables are in good agreement with measurements, nonetheless the dispersion behaviour is partially satisfactory due to wind unsteadiness which is difficult to reproduce. These results point out that the developed model is suitable for the dispersion study in a real urban canopy, despite of the differences concerning the local concentration values.

By means of our dispersion model we can simulate atmospheric flows under neutral or weakly stable stability conditions. Work is currently in progress concerning the suitability for convective conditions. As future research we consider the possibility of a grid resolution refinement in order to assess the influence of the horizontal mesh on the simulation of the dispersion processes. Ongoing research is expected to strengthen the analysis with further simulations for different experimental data sets.

ACKNOWLEDGEMENTS

This work was supported by the HPC resources of IDRIS (*Institut de Développement et de Recherche pour l'Informatique Scientifique*) under the allocation 2013010132 made by GENCI. The experimental campaigns FluxSAP 2010 and 2012 have been funded by EC2CO/INSU program in the framework of the VegDUD project. Vera Rodrigues gratefully acknowledges support from CNRS and Région des Pays de la Loire.

REFERENCES

- Borrego C., M. Maché, J.H. Amorim, J.F. Sini, H. Martins, I. Calmet, J. Valente, V. Rodrigues, A.I. Miranda, D. Maro, J.M. Rosant and C. Pimentel, 2012: Merging the gap between meso and micro scales: enhanced inflow boundary conditions for CFD modelling of urban air quality, 32nd NATO/SPS International Technical Meeting on Air Pollution Modelling and its Application (ITM2012), 7-11 May, Utrecht, The Netherlands.
- Francis M., D. Maro, O. Connan, D. Hébert, M. Goriaux, B. Letellier and P. Defenouillère, 2012: Experimental study of atmospheric 3D dispersion of a passive tracer in urban environment: Comparison with Briggs urban model, 20th International Conference on Modelling, Monitoring and Management of Air pollution (Air pollution XX), 16-18 May, A Coruña, Spain, 261-271.
- Maché M., I. Calmet, J.F. Sini and J.M. Rosant, 2012: Large-eddy simulation of urban microclimate using multi-layer canopy model, 8th International Conference on Urban Climates (ICUC8), 6-10 August, Dublin, Ireland.
- Maro, D., I. Calmet, P. Mestayer, M. Goriaux, D. Hébert, O. Connan, B. Letellier, P. Defenouillère, J.M. Rosant and V. Rodrigues, 2011: FluxSAP 2010 experimental campaign, part 2: quantification of plume vertical dispersion during a gas tracer experiment using a mast and a small tethered balloon. HARMO 14, Kos Island, Greece, 438-442.
- Rodrigues V., I. Calmet, D. Maro, M. Maché, D. Hébert, O. Connan and J.M. Rosant, 2012: Numerical and experimental tracer dispersion study for footprint assessment, 8th International Conference on Urban Climates (ICUC8), 6-10 August, Dublin, Ireland.